Regulation of bile canalicular network formation and maintenance by AMP-activated protein kinase and LKB1

Dong Fu[1], Yoshiyuki Wakabayashi[1], Yasuo Ido[2], Jennifer Lippincott-Schwartz[1] and Irwin M. Arias[1,*]

[1]Cell Biology and Metabolism Program, *Eunice Kennedy Shriver* National Institute of Child Health and Human Development, National Institute of Health, Bethesda, MD 20892, USA
[2]Department of Medicine, Section of Endocrinology, Boston University School of Medicine, Boston, MA 02118, USA
*Author for correspondence (ariasi@mail.nih.gov)

Accepted 21 June 2010
Journal of Cell Science 123, 3294-3302

doi:10.1242/jcs.068098

Summary

AMP-activated protein kinase (AMPK), a cellular metabolic sensor, is essential in energy regulation and metabolism. Hepatocyte polarization during liver development and regeneration parallels increased metabolism. The current study investigates the effects of AMPK and its upstream activator LKB1 on polarity and bile canalicular network formation and maintenance in collagen sandwich cultures of rat hepatocytes. Immunostaining for the apical protein ABCB1 and the tight junction marker occludin demonstrated that canalicular network formation is sequential and is associated with activation of AMPK and LKB1. AMPK and LKB1 activators accelerated canalicular network formation. Inhibition of AMPK or LKB1 by dominant-negative AMPK or kinase-dead LKB1 constructs blocked canalicular network formation. AICAR and 2-deoxyglucose, which activate AMPK, circumvented the inhibitory effect of kinase-dead LKB1 on canalicular formation, indicating that AMPK directly affects canalicular network formation. After the canalicular network was formed, inhibition of AMPK and LKB1 by dominant-negative AMPK or kinase-dead LKB1 constructs resulted in loss of canalicular network, indicating that AMPK and LKB1 also participate in network maintenance. In addition, activation of AMPK and LKB1 prevented low-Ca^{2+}-mediated disruption of the canalicular network and tight junctions. These studies reveal that AMPK and its upstream kinase, LKB1, regulate canalicular network formation and maintenance.

Key words: AMPK, LKB1, Bile canaliculi, Polarity, Primary hepatocytes, Collagen sandwich culture, P-glycoprotein, Tight junction

Introduction

Hepatocytes, the major epithelial cells in the liver, are polarized. Tight junction proteins, such as occludin, claudin and ZO-1, seal the canalicular lumen, separate apical and basolateral membrane domains (Kojima et al., 2003; Vinken et al., 2006) and form the bile canaliculus across which bile is secreted. Hepatocyte polarization is essential for biliary secretion. Loss of polarity causes bile secretory failure (cholestasis) and liver damage (Arias et al., 1993). The mechanisms of polarization are complex and include cytoskeletal, tight junctional and intracellular trafficking components (Bryant and Mostov, 2008; Hoekstra et al., 2004; Mostov et al., 2003; Rodriguez-Boulan et al., 2005; Rodriguez-Boulan and Salas, 1989; Wakabayashi et al., 2005).

In liver development and regeneration, hepatocyte polarization parallels changes in energy metabolism (Fausto et al., 2006; Fernandez et al., 2006; Hyatt et al., 2008), which influences many functions, including carbohydrate and lipid metabolism, proteins synthesis, detoxification, bile production and secretion. The mechanistic basis for how energy metabolism regulates hepatocyte polarization remains unclear. AMP-activated protein kinase (AMPK), a serine threonine kinase containing a catalytic α-subunit and regulatory β- and γ-subunits, controls energy metabolism within cells by sensing the cellular AMP to ATP ratio (Shackelford and Shaw, 2009). Activation of AMPK by phosphorylation of α-subunit Thr172 decreases energy consumption and increases energy production during cellular stress, such as hypoxia, isochemia and glucose deprivation (Hardie, 2007). AMPK also has an important role in hepatic metabolism through direct effects on lipid, glucose and protein homeostasis, and mitochondrial biogenesis (Viollet et al., 2009), and long-term effects on expression of genes including the glycolytic and lipogenic gene ChREBP (carbohydrate response element-binding protein) (Foretz et al., 2005) and the gluconeogenesis gene TORC2 (transducer of regulated CREB activity 2) (Koo et al., 2005). AMPK can be activated by phosphorylation of the Thr172 residue in its α-subunit by LKB1 (liver kinase B1), an upstream serine threonine kinase (Alessi et al., 2006; Forcet and Billaud, 2007). Formerly, AMPK was solely considered as a cellular sensor of AMP to ATP ratio; however, recent studies reveal that AMPK and LKB1 regulate polarity in *Drosophila*, intestinal epithelia and neurons (Amin et al., 2009; Baas et al., 2004; Barnes et al., 2007; Lee et al., 2007; Mirouse et al., 2007; Shelly et al., 2007). Given the polarity role of AMPK and LKB1, we set out to investigate whether the activity of these proteins is central to hepatocyte polarity manifested by canalicular network formation and maintenance.

A major difficulty in studying hepatocyte polarity is the lack of a cell culture system that exhibits the canalicular network structure that defines hepatocyte architecture. Previous studies used WIF-B9 or HepG2 cells, but these form only small canalicular spheres between adjacent cells rather than canalicular networks that are characteristic of hepatocytes within the liver (Gallin, 1997; Herrema et al., 2006; Theard et al., 2007; Wakabayashi et al., 2005). By contrast, collagen sandwich cultures of primary mammalian hepatocytes form a multicellular canalicular network composed of

Journal of Cell Science

non-dividing cells, as seen in vivo (Decaens et al., 2008; LeCluyse et al., 1994), and maintain this functional organization for about 2 weeks (Ben-Ze'ev et al., 1988; Dunn et al., 1989; Musat et al., 1993). Therefore, to investigate the role of AMPK and LKB1 in canalicular network formation and maintenance, we used collagen sandwich cultures of rat primary hepatocytes.

Results

Association of canalicular network formation and AMPK activation

To investigate the process of canalicular network formation in cultured rat hepatocytes, we examined the daily morphological structure of canaliculi using bright-field illumination combined with immunofluorescence of occludin, a junctional marker, and ABCB1 (P-glycoprotein), an apical marker. Canalicular shape, length and network formation, as well as the distribution of ABCB1 and occludin were recorded in cultures from day 1 through 6. As shown in Fig. 1, in day 1 cultures, canaliculi structures situated between two cells and positive for occludin and ABCB1 were infrequent and small. In day 2 cultures, canalicular number and length per cell increased, with canaliculi mainly rounded and shared by two adjacent cells (Fig. 1A–C). In day 3 cultures, canaliculi were elongated and bar-shaped.

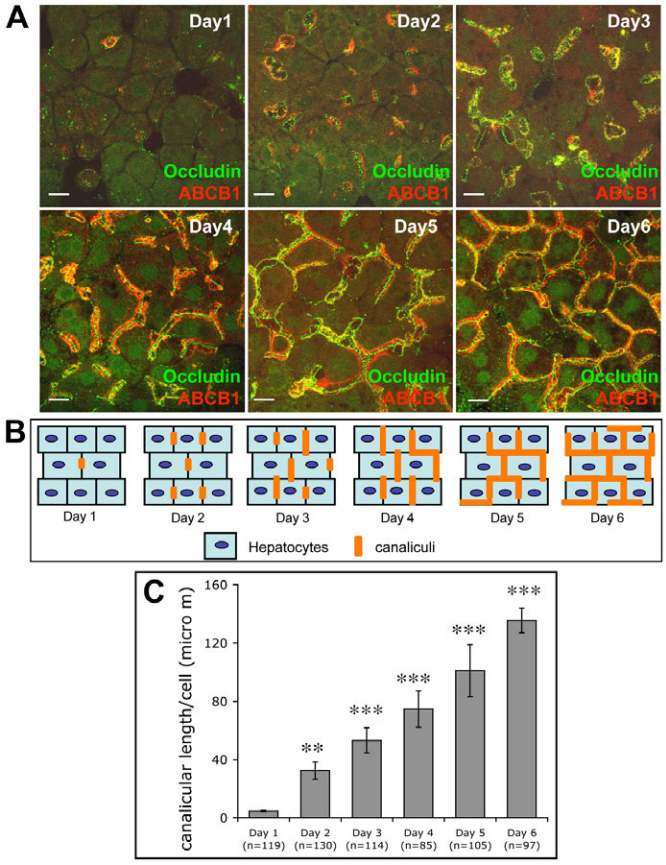

Fig. 1. Progressive canalicular network formation in sandwich cultures of rat primary hepatocytes. Immunofluorescence of the tight junction marker occludin (green) and the apical marker ABCB1 (red) was used to study canalicular structure in day 1 to day 6 cultures. Projection images are from *z*-series of confocal images. (**A**) Daily progress of canalicular network formation in sandwich culture. Scale bars: 15 µm. (**B**) Diagram of canalicular network formation. (**C**) Mean canalicular length (±s.d.) from three individual experiments (n, cell number; $^{**}P<0.01$, $^{***}P<0.001$).

The canalicular length per cell had increased significantly and now three to four cells shared each canaliculus (Fig. 1A–C). In day 4 and 5 cultures, canaliculi progressively elongated and became interconnected as tubular structures (Fig. 1A–C). In day 6 cultures, canaliculi continued to lengthen and formed an extensive branched network, which is the mature morphological form. After the fully branched network was formed in day 6 cultures, canalicular structure and length per cell remained unchanged for 14 days when cells began to deteriorate (data not shown). The sequential morphological pattern of bile canalicular network formation was reproducible and consistent.

To examine possible linkage between the metabolic sensor AMPK and canalicular network formation, western blots of total and phosphorylated Thr172 α-subunit AMPK were performed on different days during culture. Both total and phosphorylated AMPK (Thr172) levels progressively increased from day 1 to day 6 (Fig. 2A,B). On day 2, both total and phosphorylated AMPK significantly increased ($P<0.01$). By day 3, levels of total AMPK and phosphorylated AMPK increased 3.2±0.7-fold ($P<0.001$) and 2.2±0.3-fold ($P<0.001$), respectively, compared with day 1 cultures. On days 4 and 5, AMPK levels increased relative to day 1 ($P<0.05$); however, they were reduced when compared with levels on day 3. On day 6, when cells formed a branched canalicular network, total and phosphorylated AMPK increased 4.6±0.4-fold ($P<0.001$) and 2.6±0.4-fold ($P<0.001$), respectively, compared with day 1 (Fig. 2A,B). The ratio of phosphorylated to total AMPK did not significantly change from day 2 to day 5 when compared with day 1, but decreased on day 6 (Fig. 2C); however, the level of phosphorylated AMPK increased significantly in day 2 to day 6 cultures, compared with day 1 ($P<0.05$). To confirm functional activation of AMPK, total and phosphorylated acetyl-CoA carboxylase-Ser79 (ACC-Ser 79), which is an AMPK substrate, were measured by western blotting in day 1 to day 6 cultures. The ratio of phosphorylated to total ACC progressively increased, similarly to phosphorylated AMPK (Thr172) (2.9- to 7.0-fold; $P<0.01$), confirming increasing activation of AMPK during canalicular network formation (Fig. 2D,E). Because upregulation and activation of AMPK paralleled canalicular network formation, these events might be functionally related.

Overexpression of dominant-negative AMPK inhibits canalicular network formation

To determine a role for AMPK in canalicular network formation, we tested whether inactivation of AMPK inhibits canalicular network formation. Since no reliable AMPK inhibitors are available, dominant-negative (DN) AMPK adenovirus was used to inhibit AMPK activation. In day 1 cultures, hepatocytes were infected with either Myc-DN-AMPK or control GFP adenoviruses. Immunostaining for ABCB1 and Myc was performed 48 hours later. The infection rates were 5–10% for Myc-DN-AMPK and 10–20% for GFP. GFP-infected cells had similar canalicular morphology to control cells on day 3, indicating that adenovirus infection per se did not interfere with canalicular network formation (Fig. 2F). Hepatocytes overexpressing Myc-DN-AMPK mutants either lost bile canaliculi, or retained small canaliculi, resembling the morphology of day 1 cultures, and canalicular length per cell significantly decreased (Fig. 2F,G). Non-infected cells had well-developed canaliculi shared by three to four cells, which were similar to those seen in control day 3 cultures. These results indicated that canalicular formation is inhibited by overexpression of Myc-DN-AMPK, suggesting that AMPK participates in canalicular network formation.

AMPK upstream kinase, LKB1, also participates in canalicular network formation

AMPK can be activated by upstream kinases LKB1 and CaMKK (calmodulin-dependent protein kinase kinase). LKB1 is active in the liver, and CaMKK activates AMPK, mainly in the brain (Shackelford and Shaw, 2009). To examine whether LKB1 activity is also associated with canalicular network formation, western blots of total and phosphorylated LKB1 (Ser431) were performed during 6 days of culture. Although LKB1 has several phosphorylation sites, only Ser431 phosphorylation, as measured by the antibody used, facilitates active transport of LKB1 from the nucleus to cytoplasm, where it is activated (Jansen et al., 2009). Phosphorylation on Ser431 was used for indication of LKB1 activation (Shelly et al., 2007). As observed with AMPK (Fig. 2A,B), both total and phosphorylated LKB1 progressively increased from day 1 to day 6 ($P<0.05$) (Fig. 3A,B). Compared with day 1, the ratio of phosphorylated to total LKB1 was not significantly changed from day 3 to day 6, except there was decrease on day 2, which was probably due to the large increase in total LKB1 (Fig. 3C). However, phosphorylated LKB1 progressively increased from day 2 to day 6, compared with day 1. Moreover, activation of LKB1 downstream kinase AMPK, as identified by phosphorylated AMPK (Thr172) and phosphorylated ACC (Ser79), significantly increased from day 1 to day 6 (Fig. 2A,B,D,E). Collectively, upregulation and activation of LKB1 paralleled AMPK activation and canalicular network formation, suggesting that LKB1 is related to AMPK-mediated canalicular network formation.

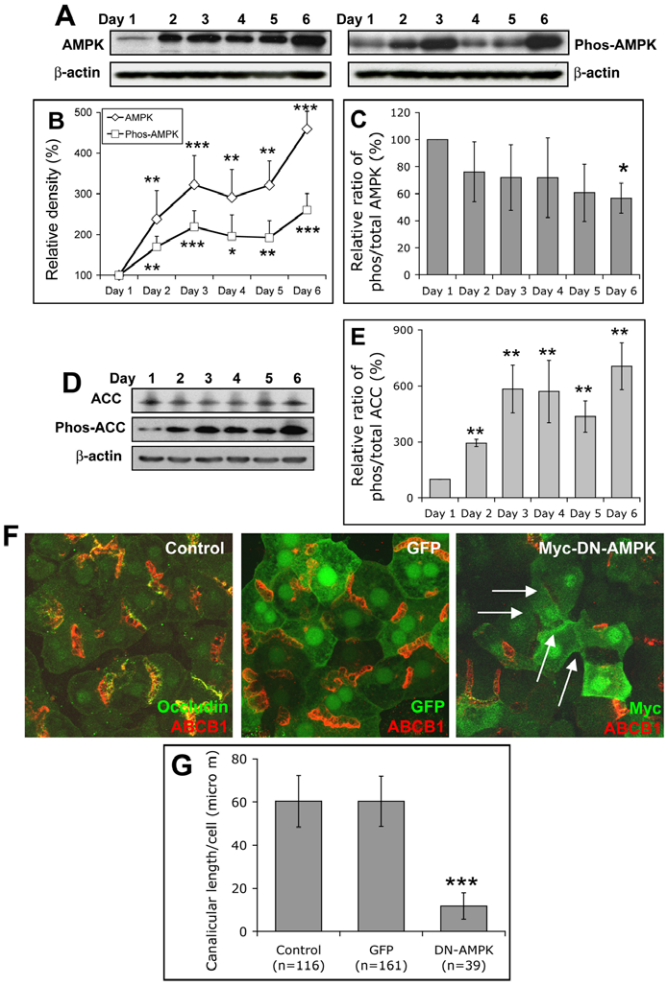

Fig. 2. AMPK activation in day 1 to day 6 cultures. Total proteins were extracted from day 1 to day 6 cultures. (**A**) Western blot for AMPK and phosphorylated AMPK (Thr172). (**B**) Mean densitometry measurements (±s.d.) from four individual experiments (*$P<0.05$, **$P<0.01$, ***$P<0.001$). (**C**) Ratio (mean ± s.d.) of phosphorylated to total AMPK (*$P<0.05$). (**D**) Western blot for total and phosphorylated ACC (Ser79) in day 1 to day 6 cultures. (**E**) Densitometry measurements for ratio of phosphorylated to total ACC (from three individual experiments; mean ± s.d.; **$P<0.01$). (**F**) Inhibitory effect of dominant-negative AMPK on canalicular network formation. In day 1 cultures, hepatocytes were infected with GFP or Myc-DN-AMPK adenoviruses. 48 hours after infection, immunostaining was performed for control cells (occludin and ABCB1), GFP cells (ABCB1) and Myc-DN-AMPK cells (Myc and ABCB1). Projection images are from *z*-series of confocal images. (**G**) Mean canalicular length per cell (± s.d. from three individual experiments; n, cell number; ***$P<0.001$).

Overexpression of kinase-dead LKB1 mutants inhibited canalicular network formation

To determine the role of upstream kinase activity of LKB1 in AMPK mediated canalicular network formation, hepatocytes were infected on day 1 with kinase-dead LKB1 (D194A, KD-LKB1) or control GFP adenoviruses, and immunostaining experiments were performed 48 hours later. The infection rates were 5–10% for KD-LKB1 and 10–20% for GFP. Hepatocytes that overexpressed KD-LKB1 mutant either lost bile canaliculi or retained small canaliculi, which resembled the morphology of day 1 cultures (Fig. 3D). GFP-infected cells and non-infected control cells had bar-shaped canaliculi shared by three to four cells, similarly to day 3 cultures (Fig. 3D). Canalicular formation was inhibited by KD-LKB1, confirming that the LKB1–AMPK pathway participates in canalicular network formation.

Because LKB1 is an upstream activator of AMPK, we tested whether direct AMPK activation rescues canalicular network formation after hepatocytes were infected with the KD-LKB mutant. Hepatocytes were treated with 5-aminoimidazole-4-carboxamide-1-b-riboside (AICAR, 500 μM, 24 hours) or 2-deoxyglucose (2-DG) (25 mM, 24 hours), which activate AMPK (Hawley et al., 2003; Hurley et al., 2005; Shackelford and Shaw, 2009), 24 hours after infection with KD-LKB1 virus. Immunostaining for LKB1 and ABCB1 revealed that KD-LKB1-infected cells formed canaliculi that were similar to those in day 3–4 cultures after activation of AMPK by AICAR or 2-DG, and non-infected cells within the same field formed a network of longer branched canaliculi similarly to day 5–6 cultures, whereas cells only expressing KD-LKB1 lost canaliculi (Fig. 3D,E). These results reveal that AICAR or 2-DG activated endogenous LKB1-AMPK and overcame the inhibitory effect of KD-LKB1 on canalicular network formation. The 2-DG effect was observed at concentrations of 25–100 mM (supplementary material Fig. S1). In addition, specific inhibition of CaMKK, an AMPK upstream kinase in brain, using STO609, had no effect on canalicular network formation (data not shown).

Activation of LKB1 and AMPK accelerates canalicular network formation

To determine whether activation of LKB1 and AMPK in day 2 cultures is sufficient to induce canalicular network formation, we tested the effect of activators of these proteins. Activators included forskolin, which stimulates LKB1 (Collins et al., 2000; Sapkota et al., 2001), AICAR and 2-DG. Western blot analysis revealed that

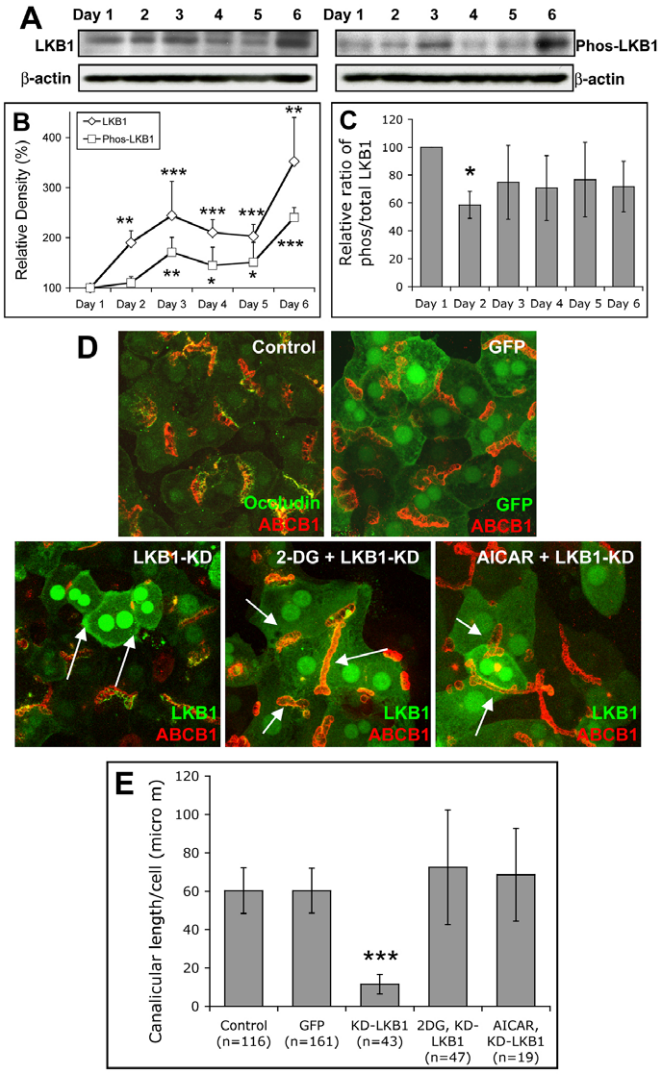

Fig. 3. LKB1 activation in day 1 to day 6 cultures. Total proteins were extracted from Day1 to day 6 cultures. (**A**) Western blot for LKB1 and phosphorylated LKB1 (Ser431). (**B**) Mean densitometry measurements (±s.d. from four individual experiments; **P*<0.05, ***P*<0.01, ****P*<0.001). (**C**) Mean ratio (±s.d.) of phosphorylated to total LKB1 (**P*<0.05). (**D**) Inhibitory effect of kinase-dead LKB1 on canalicular network formation. In day 1 cultures, hepatocytes were infected with GFP or KD-LKB1 adenoviruses. One day later, cells were treated with or without 2-DG (25 mM) or AICAR for 24 hours. Immunostaining was performed using control cells (occludin and ABCB1), GFP cells (ABCB1), KD-LKB1 cells (LKB1 and ABCB1), KD-LKB1 + 2-DG cells (LKB1, ABCB1) and KD-LKB1 + AICAR cells (LKB1, ABCB1). Projection images are from *z*-series of confocal images. Arrows indicate loss of canalicular structure between KD-LKB1 overexpressed cells (bottom left image) or prevention of loss of canalicular structure after treatment with 2-DG or AICAR (bottom middle and right images, respectively). (**E**) Mean canalicular length per cell (±s.d. from three individual experiments; n, cell number; ****P*<0.001).

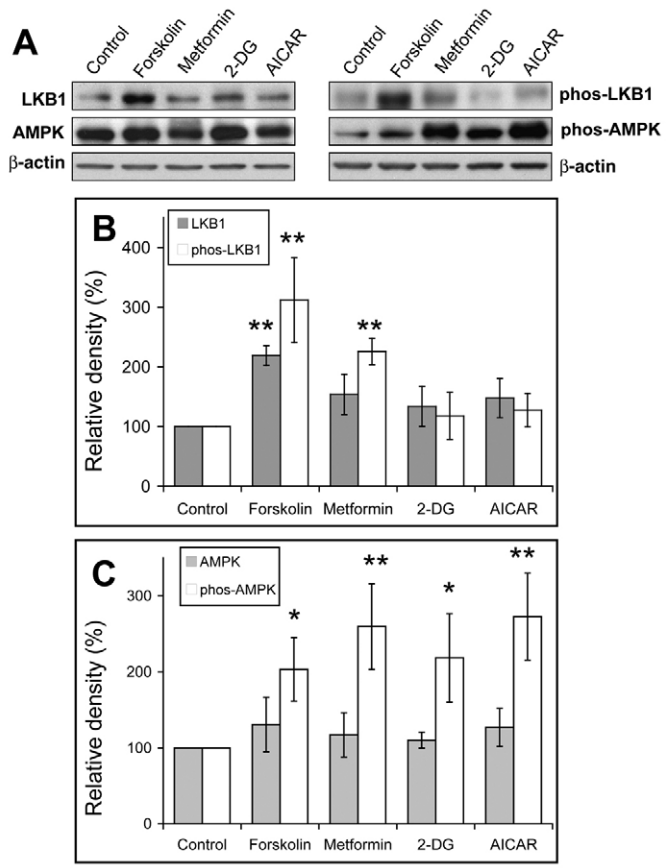

Fig. 4. Effect of AMPK and LKB1 activators on total and phosphorylated LKB1 and AMPK. (**A**) In day 2 cultures, hepatocytes were treated with forskolin (100 μM), metformin (500 μM), 2-DG (100 mM) and AICAR (500 μM) for 24 hours, respectively. Total proteins were extracted from the cells and western blots for LKB1, AMPK, phosphorylate-LKB1 (Ser431) and phosphorylated-AMPK (Thr172) were performed. (**B**,**C**) Mean densitometry measurements (±s.d. from three individual experiments; **P*<0.05, ***P*<0.01).

forskolin increased phosphorylated-LKB1 (Ser431) 3.1±0.7-fold (*P*<0.01), and its downstream phosphorylated-AMPK (Thr172) 2.0±0.4-fold (*P*<0.05) compared with the relevant controls (Fig. 4A–C). Similarly, AICAR and 2-DG increased phosphorylated AMPK (Thr172) 2.7±0.6-fold (*P*<0.01) and 2.2±0.6-fold (*P*<0.05), respectively, compared with relevant controls, and did not activate LKB1 (Fig. 4A–C). Metformin, which also activates the LKB1–AMPK pathway (Xie et al., 2008), increased phosphorylation of both LKB1 (Ser431) and AMPK (Thr172) 2.3±0.2-fold (*P*<0.001) and 2.6±0.6-fold (*P*<0.01) compared with controls (Fig. 4A–C). Forskolin also significantly increased total LKB1 levels, possibly as a result of a transcriptional effect. For AMPK, only phosphorylation changed with the various treatments, probably because 2-DG and AICAR only activate AMPK and do not alter its synthesis or degradation. Forskolin and metformin activate AMPK via LKB1 and did not affect AMPK protein levels.

Canalicular morphology was then examined by immunofluorescence for occludin and ABCB1. Twenty-four hours after day 2 cultures were treated with each activator, canaliculi were longer, branched and similar to results observed on day 5 or day 6 in non-treated cultures. Control cells on day 3 showed bar-shaped non-branching canaliculi (Fig. 5A). Activation of AMPK or LKB1 significantly increased canalicular length per cell compared with control cells (1.9–2.8-fold, *P*<0.05) (Fig. 5B). In addition, similar effects of 2-DG were observed at concentrations of 25, 50 and 100 mM (see supplementary material Fig. S2). These results demonstrate that activation of LKB1 and AMPK resulted in accelerated canalicular network formation, confirming an essential role of the LKB1–AMPK pathway in canalicular network formation.

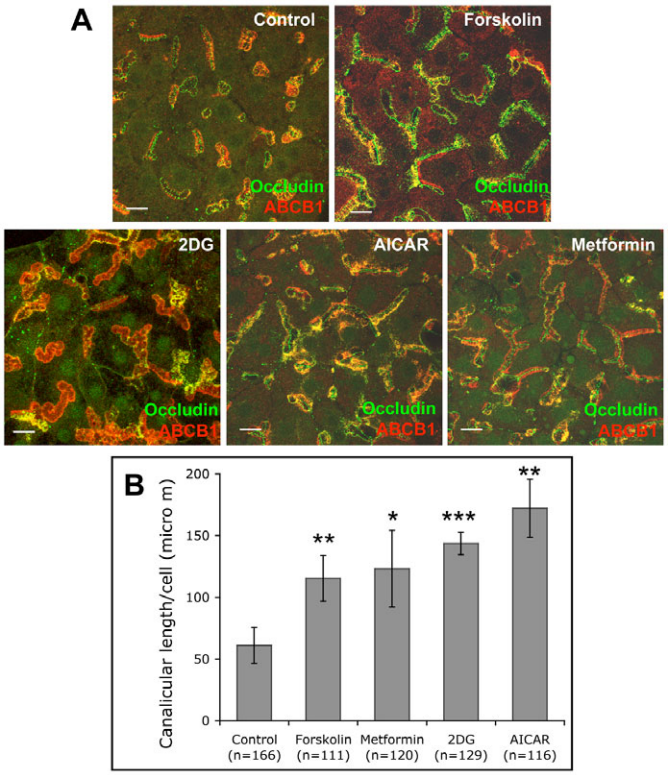

Fig. 5. Effect of AMPK and LKB1 activators on bile canalicular network formation. (**A**) Day 2 cultures were treated with forskolin (100 μM), metformin (500 μM), 2-DG (100 mM) or AICAR (500 μM) for 24 hours. Immunofluorescence of the tight junction marker occludin (green) and the apical marker, ABCB1 (red) was used to study canalicular structure. Projection images are from *z*-series of confocal images. Scale bars: 15 μm. (**B**) Mean canalicular length per cell (±s.d from three individual experiments; n, cell number; **P*<0.05, ***P*<0.01, ****P*<0.001).

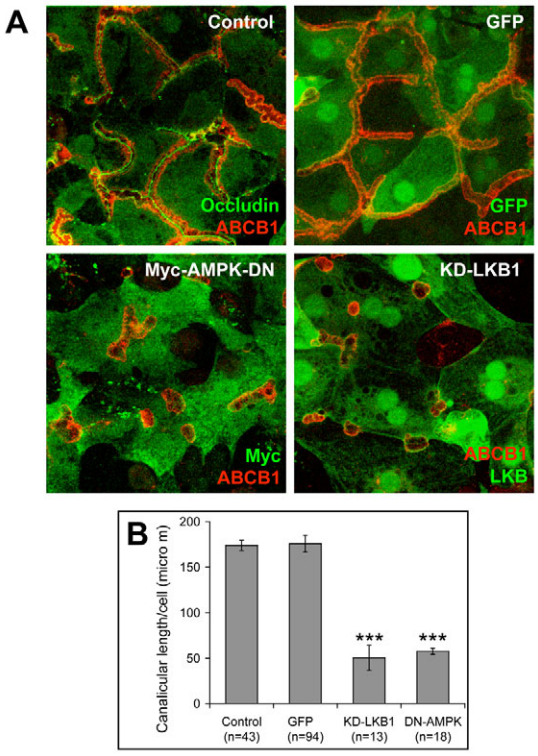

Fig. 6. Inhibitory effects of dominant-negative AMPK and kinase-dead LKB1 on canalicular network maintenance. On day 6, hepatocytes were infected with GFP, Myc-DN-AMPK and KD-LKB1 adenoviruses respectively. 72 hours after infection, immunostaining was performed for control cells (occludin and ABCB1), GFP cells (ABCB1), Myc-DN-AMPK cells (Myc and ABCB1) and KD-LKB1 cells (LKB1 and ABCB1). (**A**) Projection images from *z*-series of confocal images. (**B**) Mean canalicular length per cell ± s.d. (n, cell number; ****P*<0.001).

LKB1 and AMPK also regulate canalicular network maintenance

We further examined the role of AMPK and LKB1 activity on canalicular network maintenance after canaliculi had been fully formed. Immunostaining with occludin and ABCB1 showed that, after the fully branched network was formed in day 6 cultures, canalicular structure was unchanged up to 14 days, after which the cells deteriorated (data not shown). To access the role of LKB1 and AMPK activity in maintenance of this structure, hepatocytes at day 6 in culture were infected with Myc-DN-AMPK, KD-LKB1 or control GFP viruses. The infection rates were 10%, 10% and 20% for Myc-DN-AMPK, KD-LKB1 and GFP at 72 hours after infection, respectively, and cells remained healthy in appearance. Canalicular structure was studied by ABCB1 immunostaining 24, 48 and 72 hours after infection. Because of very low expression levels 24 hours after infection, DN-AMPK and KD-LKB1 treatment had no discernable effect on canalicular structure compared with adenovirus-GFP or control treatments (data not shown). However, at 48 or 72 hours after infection, canaliculi between cells that overexpressed either Myc-DN-AMPK or KD-LKB1 became small and round, and canalicular length per cell significantly decreased when compared with GFP or control cells (Fig. 6A,B). Canaliculi remained as a branched network in control cells or GFP-infected cells (Fig. 6). Overexpression of DN-AMPK and KD-LKB inhibited AMPK or LKB1 activity and resulted in loss of branched canalicular structure, revealing that AMPK and LKB1 also participate in canalicular network maintenance.

To further confirm the role of AMPK and LKB1 activity in canalicular network maintenance, we studied the effect on day 6 cultures of Ca^{2+} removal from the medium with and without added LKB1 or AMPK activators. Extracellular Ca^{2+} is required for cellular junction assembly. As previously observed in epithelial cell lines (Zhang et al., 2006; Zheng and Cantley, 2007), Ca^{2+} depletion in the medium caused junction fragmentation and disruption, and loss of polarity with only a few small canaliculi remaining (Fig. 7A). In addition, ABCB1 distribution decreased in the canalicular domain and accumulated intracellularly (Fig. 7A). To ensure that canalicular disruption was not due to low-Ca^{2+} toxicity, cells were switched back to normal medium for 1 day after incubation for 24 hours in low-Ca^{2+} medium. Immunostaining with ABCB1 and occludin demonstrated canalicular network restoration and similar morphology to day 6 cultures (Fig. 7A), indicating that low Ca^{2+} did not produce irreversible toxicity. The effects of LKB1 and AMPK were then tested. After cells were incubated for 24 hours in low-Ca^{2+} medium containing LKB1 or AMPK activators, there was no fragmentation of occludin or loss of apical ABCB1. LKB1 and AMPK activators prevented canalicular disruption and canaliculi retained a branched network

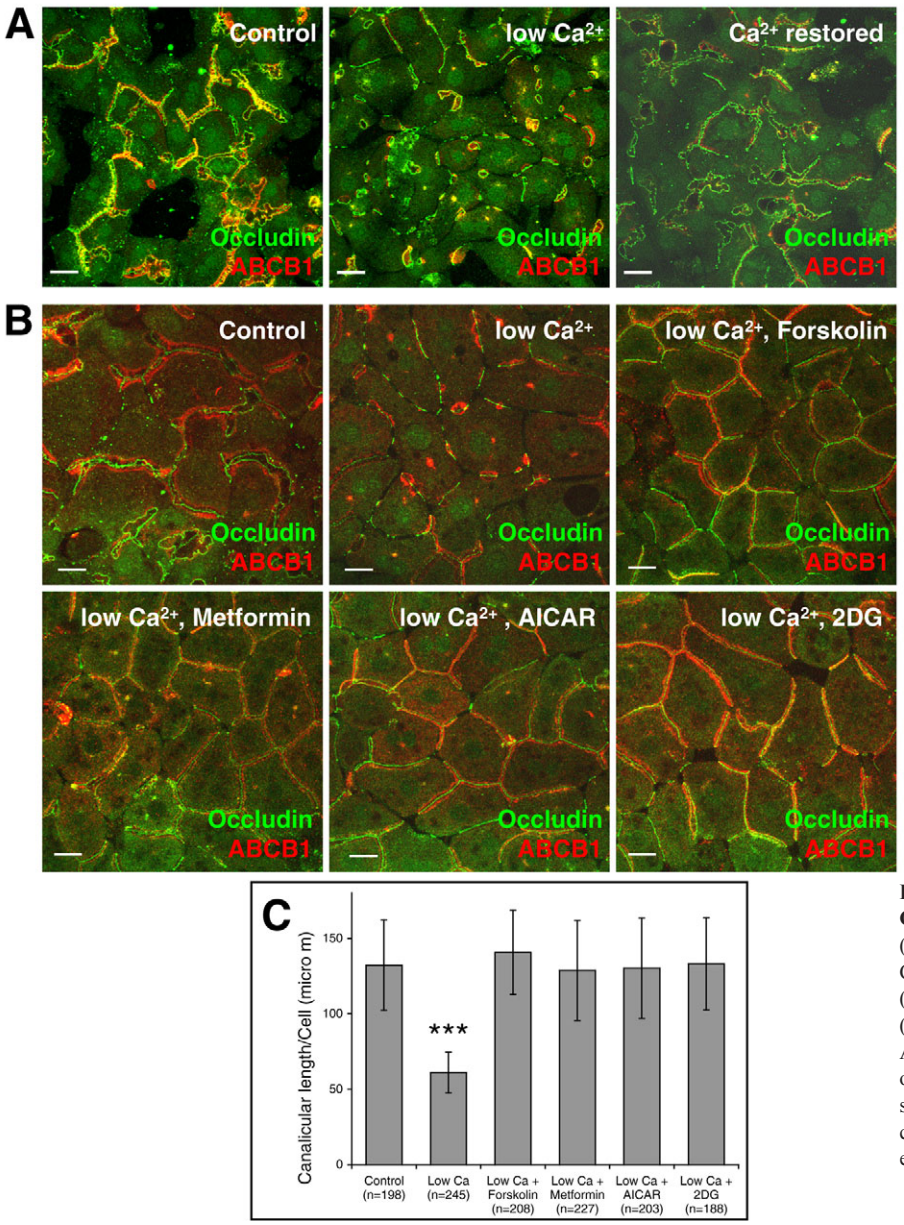

Fig. 7. AMPK and LKB1 activators prevent low-Ca^{2+}-mediated canalicular network disruption. (**A**) Low-Ca^{2+} treatment on day 6 culture for 24 hours. Cells were restored to normal medium for 24 hours. (**B**) Low-Ca^{2+} medium in the presence of forskolin (100 μM), metformin (500 μM), 2-DG (100 mM) and AICAR (500 μM) for 24 hours. Immunostaining for occludin and ABCB1. Projection images are from *z*-series of confocal images. Scale bars: 15 μm. (**C**) Mean canalicular length per cell (±s.d. from four individual experiments; n, cell number; ***$P<0.001$).

pattern typical of day 6 morphology (Fig. 7B). Measurement of canalicular length revealed that canaliculi were significantly longer after treatment with AMPK and LKB1 activators than in low-Ca^{2+} treatment alone ($P<0.001$) (Fig. 7C). The protective effects of LKB1 and AMPK activators on low-Ca^{2+}-mediated canalicular disruption confirm that activation of LKB1 and AMPK is necessary for canalicular network maintenance.

Discussion

The present study reveals an important link between AMPK, metabolism and polarity in hepatocytes. This was made possible because of the use of a collagen sandwich culture system that allows non-dividing hepatocytes to form a multicellular canalicular network that is similar to the in vivo structure, which retains normal structure and function for 2 weeks (Decaens et al., 2008). Previous studies of hepatocyte polarization used WIF-B9 and HepG2 cells (Decaens et al., 1996; Herrema et al., 2006; Theard et al., 2007), which differ from primary hepatocyte cultures because they are dividing cells and only form small non-branching canalicular spheres between adjacent cells (Decaens et al., 2008). Previous work using sandwich-cultured hepatocytes did not examine polarity, and were restricted to bright-field images or canalicular secretion of fluorescent substrates (Chandra et al., 2001; LeCluyse et al., 2000). Here, we used the sandwich-cultured hepatocytes to follow canalicular biogenesis and maintenance. We found a stepwise progression from a few canaliculi on day 1 to development of a branched canalicular network on day 6, and maintenance for at least 14 days. The reproducible sequential changes in canalicular morphology during canalicular network formation and maintenance that we observed, mimicking that seen in liver, enabled us to study its control by the LKB1–AMPK pathway.

In addition to being an important regulator of hepatic metabolism, AMPK is involved in apoptosis, proliferation, mitosis and regeneration (Hardie, 2007). Our findings reveal that AMPK and its upstream kinase, LKB1, also participate in hepatocyte polarity and canalicular network formation. Phosphorylation or activation of LKB1 and AMPK were progressively upregulated

during canalicular network formation. Comparative decreases in total and phosphorylated LKB1 and AMPK in day 4 and day 5 cultures suggest that canalicular elongation, which largely occurs during this period, might not require further kinase activation. Total AMPK and LKB1 increased during canalicular network formation, probably reflecting increased synthesis following cell isolation. Phosphorylated AMPK and LKB1 also increased as a result of activation. The ratio of phosphorylated to total LKB1 and AMPK was not increased, suggesting that the cells are not under energy stress. However, the ratio of phosphorylated to total ACC increased, confirming activation of AMPK. Overexpression of either dominant-negative AMPK or kinase-dead LKB1 mutants blocked canalicular formation. In day 2 cultures, activators of LKB1 and AMPK upregulated phosphorylation of LKB1 and AMPK, and accelerated canalicular network formation. Addition of AICAR or 2-DG to hepatocytes overexpressing KD-LKB1 rescued canalicular network formation. In our experiments, AICAR or 2-DG activated AMPK but not LKB1 (Fig. 4), which was surprising because in *Lkb1*$^{-/-}$ murine embryo fibroblasts or HeLa cells that lack LKB1, neither AICAR nor 2-DG activated AMPK (Hawley et al., 2003; Hurley et al., 2005). However, other studies suggested that AICAR activated AMPK in a LKB1-independent manner (Sakamoto et al., 2004; Sun et al., 2007). In KD-LKB1-infected cells, AICAR or 2-DG might activate endogenous LKB1, and subsequently AMPK, thereby overcoming the inhibitory effects of KD-LKB1 and rescuing canalicular network formation. This regulatory effect of AMPK and LKB1 on canalicular network formation is consistent with previous findings that LKB1 and AMPK are involved in polarity of *Drosophila*, intestinal epithelium and neurons (Amin et al., 2009; Baas et al., 2004; Lee et al., 2007; Shelly et al., 2007).

AMPK can be activated by several mechanisms in addition to AMP. In brain, CaMKK activates AMPK (Shackelford and Shaw, 2009). In sandwich-cultured hepatocytes, STO609, a specific CaMKK inhibitor, had no effect on canalicular network formation (data not shown). LKB1 also activates AMPK, and livers lacking LKB1 have reduced levels of phosphorylated AMPK (Shaw et al., 2005). The present study reveals that canalicular network formation was inhibited by overexpression of KD-LKB1, which competes with endogenous LKB1 in forming an activating heterotrimer with STRAD and MO25 (Forcet and Billaud, 2007). LKB1 can also activate MARK (microtubule-affinity-regulating kinase), the mammalian homologue of PAR1, which regulates cellular polarity (Alessi et al., 2006; Forcet and Billaud, 2007). The role of LKB1-PAR1 in hepatocyte polarity is not clear. However, our results suggest that the LKB1–AMPK pathway is essential for hepatocyte polarization.

The present study also reveals that LKB1 and AMPK participate in canalicular network maintenance. In day 6 cultures, when canaliculi were fully formed, infection with either Myc-DN-AMPK or KD-LKBl caused the fully branched canalicular network to disappear and remain only as small round canaliculi between cells overexpressing the constructs.

The exact mechanisms by which AMPK regulates canalicular formation and maintenance are not known. Previous studies in MDCK cells on the effect of low extracellular Ca^{2+} levels revealed that AMPK is involved in tight junction assembly (Zhang et al., 2006; Zheng and Cantley, 2007). Using a similar protocol, our results are consistent with the previous studies. In addition, LKB1 and AMPK activators prevented low-Ca^{2+}-induced canalicular disruption and internalization of apical protein ABCB1. AMPK possibly regulates tight junction formation by affecting the actin cytoskeleton through phosphorylation of MRLC (myosin regulatory light chain) (Mitonaka et al., 2007; Watanabe et al., 2007). In MDCK cells, WIF-B9 cells and other polarized cell lines and primary hepatocytes, the actin cytoskeleton is required for tight junction assembly and function (Hartsock and Nelson, 2008; Ivanov, 2008). In MDCK cells, mTOR is involved in AMPK-mediated tight junction assembly; however, this effect is inhibitory (Zhang et al., 2006).

An alternative mechanism for how AMPK might regulate canalicular network formation and maintenance involves apical recycling pathways. Rapid endocytic cycling of proteins and lipids to the apical membrane requires the Rab11A recycling pathway. In WIF-B9 cells (Wakabayashi et al., 2005), DN-Rab11A or motorless myosin Vb inhibited the recycling pathway and prevented polarization. These studies suggest that the Rab11a recycling system provides a polarization cue, either by delivering essential components or signaling downstream targets, such as the exocyst. In the present study, polarization and apical trafficking, as shown by ABCB1 immunostaining, occur in parallel. Because ABCB1 is no longer apical when AMPK or LKB1 is inhibited, it is likely that the recycling system is affected. The possible regulatory role of AMPK in apical recycling requires further study. Ongoing RNA microarray analysis and effects of AMPK activator and inhibitors hold promise for identifying components involved in hepatocyte polarization and thereby to clarify the role of AMPK.

Because the hepatocyte culture system studied here involves the dynamic reorganization of hepatocytes from a non-polarized to a polarized state comprised of a structured canalicular network, the regulatory information derived from its analysis might have direct bearing on normal developmental pathways. AMPK expression is required for polarization in *C. elegans*, mammalian brain and *Drosophila* (Lee et al., 2007; Narbonne and Roy, 2006; Spasic et al., 2009). Therefore, we propose that AMPK might have a similar role in embryological development of hepatocyte polarization.

Materials and Methods

Reagents and antibodies

Type-1 rat-tail collagen was from BD Biosciences (Bedford, MA). Forskolin, AICAR (5-aminoimidazole-4-carboxamide-1-b-riboside), 2-deoxyglucose (2-DG), metformin and anti-mouse IgG F(ab′)$_2$ fragment Cy3 antibody were purchased from Sigma-Aldrich. A specific mouse anti-P-glycoprotein C219 antibody which does not cross-react with ABCB11 was from Alexis Biochemicals (Plymouth Meeting, PA), rabbit anti-occludin antibody and Alexa Fluor 488 goat anti-rabbit IgG were from Invitrogen (Carlsbad, CA). Rabbit anti-acetyl coenzyme A carboxylase (ACC), mouse anti-LKB1 antibody was purchased from Abcam (Cambridge, MA). Rabbit anti-LKB1, anti-AMPK, anti-phospho-Thr172 AMPK, anti-phospho-Ser79-ACC and anti-Myc-tag antibodies were from Cell Signaling Technology (Danvers, MA). Rabbit anti-phospho-Ser431 LKB1 antibody was from Santa Cruz (Santa Cruz, CA). Peroxidase-conjugated AffiniPure Goat anti-rabbit and anti-mouse IgG were from Jackson ImmnoResearch (West Grove, PA). The ECL-Plus chemiluminescence detection system was from GE Healthcare (Piscataway, NJ).

Adenoviruses

Myc-tagged dominant-negative AMPK α1,α2 and kinase-dead mutant LKB1 (D194A, LKB1-KD) adenovirus were provided by Yasuo Ido (Boston University, Boston, MA). GFP adenovirus was provided by Erika Wittchen (University of North Carolina at Chapel Hill, CA).

Rat liver perfusion and hepatocyte isolation

As previously described (Chandra et al., 2001), male 250 g Sprague Dawley rats were anesthetized with pentobarbital intraperitoneally. Briefly, the liver was first perfused with 200 ml perfusion buffer [Krebs-Henseleit buffer (Sigma) with 0.5 μM EDTA], followed with 200 ml collagenase A buffer [Krebs-Henseleit buffer, with 0.1 mM Ca_2Cl and 0.4 mg/ml collagenase A (Sigma)]. The perfused liver was removed and separated using tweezers to release hepatocytes. After passage through 70 μm mesh, the cell solution was centrifuged at 500 r.p.m. (5 minutes, 4°C). To remove dead cells, hepatocytes were mixed with balanced Percoll solution (in Hank's buffer),

followed by centrifugation (500 r.p.m., 5 minutes, 4°C). The cell pellet was resuspended in culture medium.

Collagen sandwich hepatocyte culture

Hepatocytes were cultured in DMEM with 0.02 mg/ml insulin, 0.0284 μg/ml glucagon, 0.015 mg/ml hydrocortisone and 10% FBS. 2×10^5 freshly isolated hepatocytes were seeded in the 14 mm microwell of 35 mm glass-bottom dishes (MatTek, Ashland, MA) pre-coated with type 1 collagen (1.5 mg/ml in DMEM medium). After overnight growth, hepatocytes were overlaid with collagen and cultured in a humidified 37°C incubator in 5% CO_2 (Chandra et al., 2001). Cell density was $2.56\times10^5/cm^2$, which is similar to in vivo density ($2–3\times10^5/cm^2$) (Nakamura et al., 1984).

Low-Ca^{2+} treatment

On day 6 of culture, medium was changed to Ca^{2+}-free DMEM (0.02 mg/ml insulin, 0.0284 μg/ml glucagon, 0.015 mg/ml hydrocortisone and 10% dialyzed FBS) for 24 hours with or without various drugs. Cells were then used for immunostaining. In the Ca^{2+}-restoration experiment, low-Ca^{2+} medium was replaced with normal medium and cells were incubated for 24 hours before fixation for immunostaining.

Immunofluorescence

Sandwich cultures were fixed in 4% paraformaldehyde in PBS for 5 minutes followed by incubation with methanol for 25 minutes at –20°C (for GFP, DN-AMPK and KD-LKB1, infected cells were only fixed in 4% paraformaldehyde for 15–20 minutes), blocked and permeabilized with 1% BSA and 0.5% Triton X-100 for 1 hour, and incubated with primary antibodies overnight at 4°C. After washing with PBS, cells were incubated with anti-mouse IgG $F(ab')_2$ fragment Cy3 and/or Alexa Fluor 488 goat anti-rabbit IgG antibodies for 2 hours, followed by extensive washing in PBS. Confocal images were taken using Zeiss 510 Meta confocal microscopy with 63× oil objective and LSM 510 program (Zeiss, Oberkochen, Germany). All images were projections of *z*-stacks, and analyzed using ImageJ (NIH, Bethesda, MD). All samples were coded and scored according to morphological criteria (canalicular presence, canalicular length per cell, tight junction staining appearance and distribution of P-gp) by at least two investigators. At least three imaged areas of confluent cells were randomly selected from each culture dish. In no instance did scoring differ among investigators or samples. ImageJ was used to measure the length of canaliculi within the image field. Canalicular length was summed and divided by the number of cells to obtain the canalicular length per cell. Mean ± s.d. was calculated from three to four individual experiments.

Western blot analysis

Cultures were harvested and lysed in lysis buffer (150 mM NaCl, 1% Triton X-100, 0.1% SDS, 50 mM Tris-HCl, pH 8.0, and protease inhibitor cocktail), and sonicated 15 times for 1 second on ice, followed by centrifugation at 14,000 r.p.m. at 4°C for 30 minutes. 50 μg of total protein extracts were subjected to 8% SDS-PAGE. Following overnight transfer at 4°C for 30 minutes. PDVF membranes were blocked in 5% BSA for 1 hour, and incubated with primary antibodies overnight at 4°C. After washing in TBS-T, membranes were incubated with HRP-conjugated secondary antibody for 1 hour. After washing, proteins were detected using ECL-Plus chemiluminescence detection system. Densitometry was measured using ImageJ. Means ± s.d. were calculated from three to four individual experiments.

Statistics

Student's *t*-tests were used for analysis of densitometry and canalicular length.

The authors appreciate the advice and suggestions of Lewis Cantley (Harvard Medical School, Boston, MA), Neil Ruderman (Boston University School of Medicine, Boston, MA) and Reuben Shaw (The Salk Institute for Biological Studies, La Jolla, CA). This project was supported by the Intramural Research Program of the Eunice Kennedy Shriver National Institute of Child Health and Human Development, US National Institutes of Health. Deposited in PMC for release after 12 months.

Supplementary material available online at
http://jcs.biologists.org/cgi/content/full/123/19/3294/DC1

References

Alessi, D. R., Sakamoto, K. and Bayascas, J. R. (2006). LKB1-dependent signaling pathways. *Annu. Rev. Biochem.* **75**, 137-163.

Amin, N., Khan, A., St Johnston, D., Tomlinson, I., Martin, S., Brenman, J. and McNeill, H. (2009). LKB1 regulates polarity remodeling and adherens junction formation in the Drosophila eye. *Proc. Natl. Acad. Sci. USA* **106**, 8941-8946.

Arias, I. M., Che, M., Gatmaitan, Z., Leveille, C., Nishida, T. and St Pierre, M. (1993). The biology of the bile canaliculus, 1993. *Hepatology* **17**, 318-329.

Baas, A. F., Kuipers, J., van der Wel, N. N., Batlle, E., Koerten, H. K., Peters, P. J. and Clevers, H. C. (2004). Complete polarization of single intestinal epithelial cells upon activation of LKB1 by STRAD. *Cell* **116**, 457-466.

Barnes, A. P., Lilley, B. N., Pan, Y. A., Plummer, L. J., Powell, A. W., Raines, A. N., Sanes, J. R. and Polleux, F. (2007). LKB1 and SAD kinases define a pathway required for the polarization of cortical neurons. *Cell* **129**, 549-563.

Ben-Ze'ev, A., Robinson, G. S., Bucher, N. L. and Farmer, S. R. (1988). Cell-cell and cell-matrix interactions differentially regulate the expression of hepatic and cytoskeletal genes in primary cultures of rat hepatocytes. *Proc. Natl. Acad. Sci. USA* **85**, 2161-2165.

Bryant, D. M. and Mostov, K. E. (2008). From cells to organs: building polarized tissue. *Nat. Rev. Mol. Cell Biol.* **9**, 887-901.

Chandra, P., Lecluyse, E. L. and Brouwer, K. L. (2001). Optimization of culture conditions for determining hepatobiliary disposition of taurocholate in sandwich-cultured rat hepatocytes. *In Vitro Cell Dev. Biol. Anim.* **37**, 380-385.

Collins, S. P., Reoma, J. L., Gamm, D. M. and Uhler, M. D. (2000). LKB1, a novel serine/threonine protein kinase and potential tumour suppressor, is phosphorylated by cAMP-dependent protein kinase (PKA) and prenylated in vivo. *Biochem. J.* **345**, 673-680.

Decaens, C., Rodriguez, P., Bouchaud, C. and Cassio, D. (1996). Establishment of hepatic cell polarity in the rat hepatoma-human fibroblast hybrid WIF-B9. A biphasic phenomenon going from a simple epithelial polarized phenotype to an hepatic polarized one. *J. Cell Sci.* **109**, 1623-1635.

Decaens, C., Durand, M., Grosse, B. and Cassio, D. (2008). Which in vitro models could be best used to study hepatocyte polarity? *Biol. Cell* **100**, 387-398.

Dunn, J. C., Yarmush, M. L., Koebe, H. G. and Tompkins, R. G. (1989). Hepatocyte function and extracellular matrix geometry: long-term culture in a sandwich configuration. *FASEB J.* **3**, 174-177.

Fausto, N., Campbell, J. S. and Riehle, K. J. (2006). Liver regeneration. *Hepatology* **43**, S45-S53.

Fernandez, M. A., Albor, C., Ingelmo-Torres, M., Nixon, S. J., Ferguson, C., Kurzchalia, T., Tebar, F., Enrich, C., Parton, R. G. and Pol, A. (2006). Caveolin-1 is essential for liver regeneration. *Science* **313**, 1628-1632.

Forcet, C. and Billaud, M. (2007). Dialogue between LKB1 and AMPK: a hot topic at the cellular pole. *Sci. STKE* **2007**, pe51.

Foretz, M., Ancellin, N., Andreelli, F., Saintillan, Y., Grondin, P., Kahn, A., Thorens, B., Vaulont, S. and Viollet, B. (2005). Short-term overexpression of a constitutively active form of AMP-activated protein kinase in the liver leads to mild hypoglycemia and fatty liver. *Diabetes* **54**, 1331-1339.

Gallin, W. J. (1997). Development and maintenance of bile canaliculi in vitro and in vivo. *Microsc. Res. Tech.* **39**, 406-412.

Hardie, D. G. (2007). AMP-activated/SNF1 protein kinases: conserved guardians of cellular energy. *Nat. Rev. Mol. Cell Biol.* **8**, 774-785.

Hartsock, A. and Nelson, W. J. (2008). Adherens and tight junctions: structure, function and connections to the actin cytoskeleton. *Biochim. Biophys. Acta* **1778**, 660-669.

Hawley, S. A., Boudeau, J., Reid, J. L., Mustard, K. J., Udd, L., Makela, T. P., Alessi, D. R. and Hardie, D. G. (2003). Complexes between the LKB1 tumor suppressor, STRAD alpha/beta and MO25 alpha/beta are upstream kinases in the AMP-activated protein kinase cascade. *J. Biol.* **2**, 28.

Herrema, H., Czajkowska, D., Theard, D., van der Wouden, J. M., Kalicharan, D., Zolghadr, B., Hoekstra, D. and van Ijzendoorn, S. C. (2006). Rho kinase, myosin-II, and p42/44 MAPK control extracellular matrix-mediated apical bile canalicular lumen morphogenesis in HepG2 cells. *Mol. Biol. Cell* **17**, 3291-3303.

Hoekstra, D., Tyteca, D. and van, I. S. C. (2004). The subapical compartment: a traffic center in membrane polarity development. *J. Cell Sci.* **117**, 2183-2192.

Hurley, R. L., Anderson, K. A., Franzone, J. M., Kemp, B. E., Means, A. R. and Witters, L. A. (2005). The Ca^{2+}/calmodulin-dependent protein kinase kinases are AMP-activated protein kinase kinases. *J. Biol. Chem.* **280**, 29060-29066.

Hyatt, M. A., Budge, H. and Symonds, M. E. (2008). Early developmental influences on hepatic organogenesis. *Organogenesis* **4**, 170-175.

Ivanov, A. I. (2008). Actin motors that drive formation and disassembly of epithelial apical junctions. *Front. Biosci.* **13**, 6662-6681.

Jansen, M., Ten Klooster, J. P., Offerhaus, G. J. and Clevers, H. (2009). LKB1 and AMPK family signaling: the intimate link between cell polarity and energy metabolism. *Physiol. Rev.* **89**, 777-798.

Kojima, T., Yamamoto, T., Murata, M., Chiba, H., Kokai, Y. and Sawada, N. (2003). Regulation of the blood-biliary barrier: interaction between gap and tight junctions in hepatocytes. *Med. Electron. Microsc.* **36**, 157-164.

Koo, S. H., Flechner, L., Qi, L., Zhang, X., Screaton, R. A., Jeffries, S., Hedrick, S., Xu, W., Boussouar, F., Brindle, P. et al. (2005). The CREB coactivator TORC2 is a key regulator of fasting glucose metabolism. *Nature* **437**, 1109-1111.

LeCluyse, E. L., Audus, K. L. and Hochman, J. H. (1994). Formation of extensive canalicular networks by rat hepatocytes cultured in collagen-sandwich configuration. *Am. J. Physiol.* **266**, C1764-C1774.

LeCluyse, E. L., Fix, J. A., Audus, K. L. and Hochman, J. H. (2000). Regeneration and maintenance of bile canalicular networks in collagen-sandwiched hepatocytes. *Toxicol. In Vitro* **14**, 117-132.

Lee, J. H., Koh, H., Kim, M., Kim, Y., Lee, S. Y., Karess, R. E., Lee, S. H., Shong, M., Kim, J. M., Kim, J. et al. (2007). Energy-dependent regulation of cell structure by AMP-activated protein kinase. *Nature* **447**, 1017-1020.

Mirouse, V., Swick, L. L., Kazgan, N., St Johnston, D. and Brenman, J. E. (2007). LKB1 and AMPK maintain epithelial cell polarity under energetic stress. *J. Cell Biol.* **177**, 387-392.

Mitonaka, T., Muramatsu, Y., Sugiyama, S., Mizuno, T. and Nishida, Y. (2007). Essential roles of myosin phosphatase in the maintenance of epithelial cell integrity of Drosophila imaginal disc cells. *Dev. Biol.* **309**, 78-86.

Mostov, K., Su, T. and ter Beest, M. (2003). Polarized epithelial membrane traffic: conservation and plasticity. *Nat. Cell Biol.* **5**, 287-293.

Musat, A. I., Sattler, C. A., Sattler, G. L. and Pitot, H. C. (1993). Reestablishment of cell polarity of rat hepatocytes in primary culture. *Hepatology* **18**, 198-205.

Nakamura, T., Nakayama, Y., Teramoto, H., Nawa, K. and Ichihara, A. (1984). Loss of reciprocal modulations of growth and liver function of hepatoma cells in culture by contact with cells or cell membranes. *Proc. Natl. Acad. Sci. USA* **81**, 6398-6402.

Narbonne, P. and Roy, R. (2006). Inhibition of germline proliferation during C. elegans dauer development requires PTEN, LKB1 and AMPK signalling. *Development* **133**, 611-619.

Rodriguez-Boulan, E. and Salas, P. J. (1989). External and internal signals for epithelial cell surface polarization. *Annu. Rev. Physiol.* **51**, 741-754.

Rodriguez-Boulan, E., Kreitzer, G. and Musch, A. (2005). Organization of vesicular trafficking in epithelia. *Nat. Rev. Mol. Cell Biol.* **6**, 233-247.

Sakamoto, K., Goransson, O., Hardie, D. G. and Alessi, D. R. (2004). Activity of LKB1 and AMPK-related kinases in skeletal muscle: effects of contraction, phenformin, and AICAR. *Am. J. Physiol. Endocrinol. Metab.* **287**, E310-E317.

Sapkota, G. P., Kieloch, A., Lizcano, J. M., Lain, S., Arthur, J. S., Williams, M. R., Morrice, N., Deak, M. and Alessi, D. R. (2001). Phosphorylation of the protein kinase mutated in Peutz-Jeghers cancer syndrome, LKB1/STK11, at Ser431 by p90(RSK) and cAMP-dependent protein kinase, but not its farnesylation at Cys(433), is essential for LKB1 to suppress cell vrowth. *J. Biol. Chem.* **276**, 19469-19482.

Shackelford, D. B. and Shaw, R. J. (2009). The LKB1-AMPK pathway: metabolism and growth control in tumour suppression. *Nat. Rev. Cancer* **9**, 563-575.

Shaw, R. J., Lamia, K. A., Vasquez, D., Koo, S. H., Bardeesy, N., Depinho, R. A., Montminy, M. and Cantley, L. C. (2005). The kinase LKB1 mediates glucose homeostasis in liver and therapeutic effects of metformin. *Science* **310**, 1642-1646.

Shelly, M., Cancedda, L., Heilshorn, S., Sumbre, G. and Poo, M. M. (2007). LKB1/STRAD promotes axon initiation during neuronal polarization. *Cell* **129**, 565-577.

Spasic, M. R., Callaerts, P. and Norga, K. K. (2009). AMP-activated protein kinase (AMPK) molecular crossroad for metabolic control and survival of neurons. *Neuroscientist* **15**, 309-316.

Sun, Y., Connors, K. E. and Yang, D. Q. (2007). AICAR induces phosphorylation of AMPK in an ATM-dependent, LKB1-independent manner. *Mol. Cell. Biochem.* **306**, 239-45.

Theard, D., Steiner, M., Kalicharan, D., Hoekstra, D. and van Ijzendoorn, S. C. (2007). Cell polarity development and protein trafficking in hepatocytes lacking E-cadherin/beta-catenin-based adherens junctions. *Mol. Biol. Cell* **18**, 2313-2321.

Vinken, M., Papeleu, P., Snykers, S., De Rop, E., Henkens, T., Chipman, J. K., Rogiers, V. and Vanhaecke, T. (2006). Involvement of cell junctions in hepatocyte culture functionality. *Crit. Rev. Toxicol.* **36**, 299-318.

Viollet, B., Guigas, B., Leclerc, J., Hebrard, S., Lantier, L., Mounier, R., Andreelli, F. and Foretz, M. (2009). AMP-activated protein kinase in the regulation of hepatic energy metabolism: from physiology to therapeutic perspectives. *Acta Physiol.* **196**, 81-98.

Wakabayashi, Y., Dutt, P., Lippincott-Schwartz, J. and Arias, I. M. (2005). Rab11a and myosin Vb are required for bile canalicular formation in WIF-B9 cells. *Proc. Natl. Acad. Sci. USA* **102**, 15087-15092.

Watanabe, T., Hosoya, H. and Yonemura, S. (2007). Regulation of myosin II dynamics by phosphorylation and dephosphorylation of its light chain in epithelial cells. *Mol. Biol. Cell* **18**, 605-616.

Xie, Z., Dong, Y., Scholz, R., Neumann, D. and Zou, M. H. (2008). Phosphorylation of LKB1 at serine 428 by protein kinase C-zeta is required for metformin-enhanced activation of the AMP-activated protein kinase in endothelial cells. *Circulation* **117**, 952-962.

Zhang, L., Li, J., Young, L. H. and Caplan, M. J. (2006). AMP-activated protein kinase regulates the assembly of epithelial tight junctions. *Proc. Natl. Acad. Sci. USA* **103**, 17272-17277.

Zheng, B. and Cantley, L. C. (2007). Regulation of epithelial tight junction assembly and disassembly by AMP-activated protein kinase. *Proc. Natl. Acad. Sci. USA* **104**, 819-822.